BIOCHEMISTRY
including biophysical chemistry & molecular biology

Article

pubs.acs.org/biochemistry

Poly(A)-Binding Protein Increases the Binding Affinity and Kinetic Rates of Interaction of Viral Protein Linked to Genome with Translation Initiation Factors eIFiso4F and eIFiso4F·4B Complex

Mateen A. Khan and Dixie J. Goss*

Department of Chemistry and Biochemistry, Hunter College of the City University of New York, New York, New York 10065, United States

ABSTRACT: VPg of turnip mosaic virus (TuMV) was previously shown to interact with translation initiation factor eIFiso4F and play an important role in mRNA translation [Khan, M. A., et al. (2008) *J. Biol. Chem. 283*, 1340−1349]. VPg competed with cap analogue for eIFiso4F binding and competitively inhibited cap-dependent translation and enhanced cap-independent translation to give viral RNA a significant competitive advantage. To gain further insight into the cap-independent process of initiation of protein synthesis, we examined the effect of PABP and/or eIF4B on the equilibrium and kinetics of binding of VPg to eIFiso4F. Equilibrium data showed the addition of PABP and/or eIF4B to eIFiso4F increased the binding affinity for VPg (K_d = 24.3 ± 1.6 nM) as compared to that with eIFiso4F alone (K_d = 81.3 ± 0.2.4 nM). Thermodynamic parameters showed that binding of VPg to eIFiso4F was enthalpy-driven and entropy-favorable with the addition of PABP and/or eIF4B. PABP and eIF4B decreased the entropic contribution by 67% for binding of VPg to eIFiso4F. The decrease in entropy involved in the formation of the eIFiso4F·4B·PABP-VPg complex suggested weakened hydrophobic interactions for complex formation and an overall conformational change. The kinetic studies of eIFiso4F with VPg in the presence of PABP and eIF4B show 3-fold faster association (k_2 = 182 ± 9.0 s^{-1}) compared to that with eIFiso4F alone (k_2 = 69.0 ± 1.5 s^{-1}) . The dissociation rate was 3-fold slower (k_{-2} = 6.5 ± 0.43 s^{-1}) for eIFiso4F with VPg in the presence of PABP and eIF4B (k^{-2} = 19.0 ± 0.9 s^{-1}). The addition of PABP and eIF4B decreased the activation energy of eIFiso4F with VPg from 81.0 ± 3.0 to 44.0 ± 2.4 kJ/mol. This suggests that the presence of both proteins leads to a rapid, stable complex, which serves to sequester initiation factors.

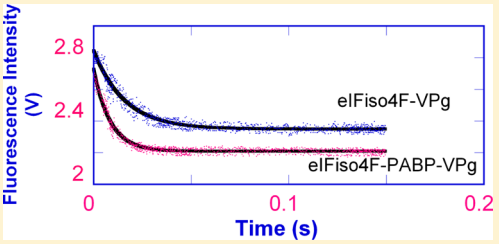

Initiation of protein synthesis in cellular mRNA involves the interaction of eIF4E (subunit of eIF4F) with the 5′-m^7G cap and the interaction of poly(A)-binding protein (PABP) with the poly(A) tail,[1] and the interaction of both proteins with eIF4G (subunit of eIF4F). eIFiso4F, an isoform of eIF4F present in higher plants,[2,3] has two subunits, eIFiso4E and eIFiso4G, and participates in similar interactions[2,3] as eIF4F subunits. eIF4G recruits eIF4A helicase and eIF3 multisubunit factors, which simultaneously associate with the 40S ribosomal subunit and promote mRNA translation.[4] Wheat germ eIFiso4F can substitute for mammalian eIF4F in an RNA-dependent ATPase activity and in cross-linking of mammalian eIF4A to the cap of oxidized mRNA.[5] Wheat germ cap-associated proteins have a very high affinity for PABP in the absence of poly(A)[6] but require poly(A) in yeast.[7] Binding of eIF4F, eIF4B, and eIF4A is believed to catalyze the efficient unwinding of secondary structure in the 5′-untranslated region.[8] In combination with PABPs, these factors promote the functional circularization of mRNA necessary for efficient translation.[4,9−12] eIF4G and eIF4B not only individually increase the binding affinity of PABP for poly(A) RNA but also together exert a synergistic effect on PABP activity,[6] which indicates that the physical interaction among all three proteins serves to stabilize their association with their respective binding sites to improve their function during translation initiation.

Potyviruses have a small protein, viral protein linked to genome (VPg), covalently attached to the 5′-end of mRNA instead of an m^7G cap structure. Potyviruses employ different strategies for preferential translation of their mRNAs through a cap-independent mechanism. It has been suggested that VPg functions like the cap structure of eukaryotic mRNA, recruiting initiation factors and 40S ribosomal subunits to viral mRNA in preference to cellular mRNA.[13,14] Interaction between VPg and eIFiso4E is critical for viral infection.[15−17] VPg interferes with the cap binding ability of eIFiso4E, resulting in the interruption of the formation of the translation initiation complex.[18] VPg has also been implicated indirectly in cell to cell movement of the virus through plasmodesmata and more directly implicated by mutagenesis in the long distance translocation of the virus.[19−21] Additionally, VPg has been shown to be the avirulence factor for recessive resistance genes in various plants.[22,23] VPg has several suggested roles in the virus life cycle. Interactions of VPg with the viral RNA polymerase in yeast[24,25] and in vitro[26] support a role in viral RNA synthesis. These observations suggest that interaction of VPg with eIFiso4F is an important step in viral protein synthesis. Earlier studies[13,14,18] have shown

Received: December 28, 2011
Revised: February 1, 2012
Published: February 2, 2012

that VPg competes with binding of cap to eIFiso4F and VPg and eIFiso4F form a stable complex. However, whether PABP affects the binding of VPg with eIFiso4F as it does for binding of m^7G cap to eIFiso4F has not been established. To examine the role of VPg in viral translation initiation, we further investigated the effect of PABP and eIF4B on the equilibrium and kinetics of binding of VPg to eIFiso4F. Addition of PABP and eIF4B increased the binding affinity of eIFiso4F for VPg. Thermodynamic studies showed a reduction in entropy for the formation of the eIFiso4F·4B·PABP complex with VPg, suggesting weakened hydrophobic interactions for complex formation and a conformational change propagated to the eIFiso4F binding site. Further, the addition of PABP increased the association rate and decreased the dissociation rate for the binding of eIFiso4F and eIFiso4F·4B with VPg. Addition of PABP decreased the activation energy of binding of VPg to eIFiso4F. These results further support the importance of the interaction of PABP and eIF4B with eIFiso4F and VPg for efficient translation.

EXPERIMENTAL PROCEDURES

Materials. Glutathione Sepharose 4B and m^7GTP-Sepharose were purchased from Amersham Biosciences Co. Ltd. Ni-NTA Superflow was purchased from Qiagen K.K. The HiTrap Mono-Q column, HiTrap SP column, and PreScission Protease were purchased from Amersham Pharmacia Biotech. Inc. The pET21a and pET28a expression vectors were purchased from Novagen, an affiliate of Merck Co. Ltd.

Preparation of Proteins. The TuMV full-length cDNA clone and construction of the expression vector for VPg were described previously.[18,27] The recombinant proteins, eIFiso4E and eIFiso4G, were expressed in *Escherichia coli* containing the constructed pET3d vector in BL21(DE3) pLysS as described previously.[28] A HiTrap Mono-Q ion exchange and m^7GTP-Sepharose columns were used for the purification of eIFiso4E. The fractions were analyzed by 12.5% sodium dodecyl sulfate–polyacrylamide gel electrophoresis. A HiTrap SP column was used to purify eIFiso4G as described previously.[28] eIF4B was expressed in *E. coli* containing the constructed pET3d vector in BL21(DE3) pLysS as described previously.[28,29] PABP was expressed in *E. coli* containing the constructed pET19b vector in BL21(DE3) pLysS as described previously.[29,30] The purity of protein was confirmed by 12% sodium dodecyl sulfate–polyacrylamide gel electrophoresis with Coomassie Brilliant Blue staining.

All protein samples were dialyzed against titration buffer [20 mM HEPES/KOH (pH 7.6), 150 mM KCl, 1.0 mM $MgCl_2$, and 1.0 mM DTT] and passed through a 0.22 μM filter (Millipore) before the spectroscopy measurements were performed. The samples were concentrated with a Centricon 10 (Amicon Co.) as necessary. The concentrations of protein were determined by a Bradford assay with bovine serum albumin as the standard[31] using a Bio-Rad protein assay reagent (Bio-Rad Laboratories).

Steady State Fluorescence Analysis. Fluorescence measurements were performed using a Spex Fluorolog τ2 spectrofluorimeter equipped with excitation and emission polarizers. The formation of the protein–protein complex was measured by direct protein fluorescence. The excitation wavelength for eIFiso4F was 280 nm, and emission was monitored at 332 nm. The excitation and emission slits were set to 4 and 5 nm, respectively. The excitation slits were chosen to prevent photobleaching, and the absorbance of the sample at the excitation wavelength was <0.02 to minimize the inner filter effect. Emission spectra were corrected for the wavelength-dependent lamp intensity and monochromator sensitivities; 100 nM eIFiso4F and eIFiso4F complexes (eIFiso4F·4B, eIFiso4F·PABP, and eIFiso4F·4B·PABP) were incubated with varying concentrations of VPg (0.0–800 nM) in titration buffer. For each data point, three samples were prepared. The fluorescence intensity of a solution containing 100 nM eIFiso4F or eIFiso4F complex was measured. A second sample with a specific amount of VPg protein was also measured, and the corrected intensities of the two samples were summed together (F_s). A third sample containing the same amount of eIFiso4F or eIFiso4F complex and VPg was mixed together, and the corrected fluorescence intensity of this complex was measured (F_c). The difference in fluorescence intensity related to the complex was defined as $\Delta F = F_c - F_s$. The normalized fluorescence difference ($\Delta F/\Delta F_{max}$) between the eIF's VPg complex was used to determine the equilibrium dissociation constant (K_d). A double-reciprocal plot was used for the determination of ΔF_{max}. Details of the data fitting are described elsewhere.[13,32,33] Fluorescence intensities were corrected for dilution, as needed, and for the inner filter effect; maximal dilutions were <7%. Nonlinear least-squares fitting of the data used KaleidaGraph version 2.1.3 (Abelbeck Software).

For formation of the complex of eIFiso4F with eIF4B and PABP, K_d values[6,34] for these interactions were used to calculate concentrations so that more than 90% of the eIFiso4F was in complex (eIFiso4F·4B, eIFiso4F·PABP, and eIFiso4F·4B·PABP) at the lowest protein mixing concentration, 100 nM. The molar ratio of eIFiso4F to eIF4B or PABP in the binding reaction mixture was 1:10; the eIFiso4F:4B:PABP ratio was 1:10:30, and the concentrations were 1, 10, and 30 μM. eIF4B and PABP were used in excess to ensure that eIF4B and PABP formed a complex with eIFiso4F, as eIF4B and PABP showed very low binding affinity for VPg. The samples were incubated for 15 min prior to titration.

To study the temperature dependence of interaction of eIFiso4F with VPg in the presence of eIF4B and PABP, the samples were thermostatically adjusted at different temperatures. The temperature was measured using a thermocouple device inside the cuvette.

Thermodynamic parameters, enthalpy (ΔH), entropy (ΔS), and free energy (ΔG), of binding of eIFiso4F and eIFiso4F complex to VPg were determined using the following equations.

$$-\ln K_{eq} = \Delta H/RT - \Delta S/R \quad (1)$$

$$\Delta G = -RT \ln K_{eq} \quad (2)$$

R and T are the universal gas constant and absolute temperature, respectively. K_{eq}, the association equilibrium constant, was determined at different temperatures (5, 10, 15, and 25 °C). ΔH and ΔS were determined from the slope and intercept, respectively, of the plot of $\ln K_{eq}$ versus $1/T$. ΔG was determined at 25 °C using eq 2.

Stopped-Flow Fluorescence Analysis. Stopped-flow fluorescence measurements were performed on an Olis RSM 1000 stopped-flow system with a dead time of 1 ms. The excitation wavelength was 280 nm, and the cut-on filter was 324 nm for eIFiso4F with VPg interactions. A reference photomultiplier was used to monitor fluctuations in lamp intensity. The temperature of the flow cell and solution reservoirs was maintained using a temperature-controlled circulating water

bath. VPg binding induced a decrease in eIFiso4F or eIFiso4F complex fluorescence. After 0.5 μM (final concentration of 0.25 μM) eIFiso4F or eIFiso4F complexes (eIFiso4F·4B, eIFiso4F·PABP, and eIFiso4F·4B·PABP) had been rapidly mixed with 5 μM (final concentration of 2.5 μM) VPg, the time course of the fluorescence intensity change was recorded by computer data acquisition. In each experiment, 1000 pairs of data were recorded, and sets of data from five to seven shots were averaged to improve the signal:noise ratio. Each averaged set of stopped-flow fluorescence data was then fit to nonlinear analytical equations using Global analysis software provided by Olis. Data were fit to the single- and double-exponential functions. Fitted curves correspond to the single-exponential equation[35]

$$F_t = \Delta F \exp(-k_{obs}\, t) + F_\infty \quad (3)$$

where F_t is the fluorescence observed at any time, t, the fluorescence when the reaction achieves equilibrium, F_∞, is the final value of fluorescence, and k_{obs} is the observed first-order rate constant. For double-exponential fits, the kinetic data were fit to the equation

$$F_t = \Delta F_1 \exp(-k_{obs1} t) + \Delta F_2 \exp(-k_{obs2} t) + F_\infty \quad (4)$$

where ΔF_1 and ΔF_2 are the amplitudes for the first and second components of the two exponentials with rate constants of k_{obs1} and k_{obs2}, respectively. The residuals were measured by the differences between the calculated fit and the experimental data. The derived rate constants were used to construct an Arrhenius plot according to the equation

$$\ln k = -\frac{E_a}{RT} + \ln A \quad (5)$$

where k is the rate constant, E_a is the activation energy, and A is the Arrhenius pre-exponential term. The activation energy was calculated from the slope of the fitted linear plot of ln k versus $1/T$ (kelvin).

Measurements of Dissociation Rate Constants. To measure the dissociation rate constants, eIFiso4F and eIFiso4F complexes (eIFiso4F·4B, eIFiso4F·PABP, and eIFiso4F·4B·PABP) with VPg were rapidly diluted 15-fold in a spectrofluorimeter cuvette, and the resulting increase in fluorescence was measured. Because of the high binding affinity of the protein−protein complex, a large dilution, which could not be accomplished by stopped-flow methods, was necessary. The concentrations of the reactants before mixing were 10 μM VPg and 2 μM eIFiso4F complex. The dissociation rates were determined from fits of the appropriate equations to the data using nonlinear least-squares fitting program KaleidaGraph version 2.1.3 (Abelbeck Software).

RESULTS

PABP Enhances the Binding Affinity of eIFiso4F and eIFiso4F·4B for VPg. We have previously[13,14] shown that eIFiso4F binds with VPg of turnip mosaic virus (TuMV). Here, we examined the effects of eIF4B and PABP on the interaction of eIFiso4F with VPg. PABP increased the binding affinity of eIFiso4F for VPg ~2.5-fold (eIFiso4F·PABP-VPg, K_d = 29.4 ± 2.0 nM; eIFiso4F-VPg, K_d = 81.3 ± 2.4 nM) at 25 °C (Figure 1). eIF4B does not affect the binding affinity of eIFiso4F and VPg (Table 1). The binding affinity of PABP alone (K_d = 1789 ± 97 nM) with VPg was much lower as shown in Table 1. On the other hand, no interaction was observed between eIF4B and VPg

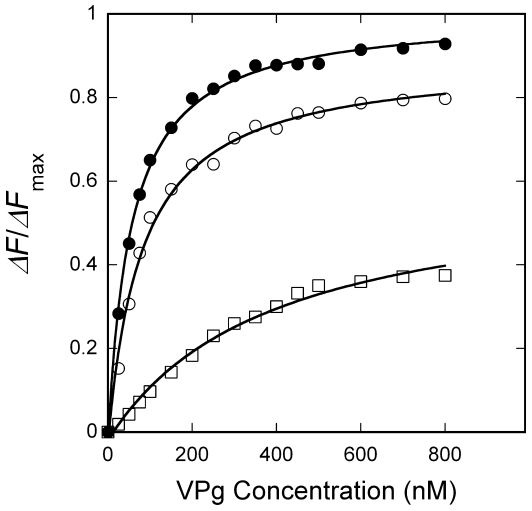

Figure 1. Poly(A)-binding protein enhances the binding affinity of eIFiso4F for VPg. Fluorescence titrations of eIFiso4F (○), eIFiso4F·-PABP (●), and PABP (□) with VPg by monitoring the intrinsic protein fluorescence intensity. The initiation factor concentration was 100 nM in titration buffer at 25 °C. The excitation and emission wavelengths were 280 and 332 nm, respectively. The curves were fit to obtain dissociation constants (K_d) as described in Experimental Procedures. The solid lines are the fitted curves. The eIFiso4F·PABP (1:10) complex were prepared by incubation of 1 μM eIFiso4F and 10 μM PABP for 15 min at 4 °C, and 90% of the protein sample was in complex form for the 100 nM titration.

(Figure 2). The titration curves in Figures 1 and 2 show the difference in fluorescence intensity between the protein−protein complex and the sum of the individual fluorescence intensities. From such analysis, the equilibrium binding constant can be calculated for the interactions between eIFiso4F and eIFiso4F complex with VPg (Table 1). eIFiso4F showed a strong interaction with VPg in the presence of PABP and eIF4B. A van't Hoff plot of ln K_{eq} versus the reciprocal of temperature (T^{-1}) was used to calculate the thermodynamic parameters, entropy (ΔS) and enthalpy (ΔH) (Table 2 and Figure 3). The values of ΔH and ΔS were obtained from the slope and intercept, respectively. The van't Hoff analyses showed that binding of VPg to eIFiso4F·PABP, eIFiso4F·eIF4B, and eIFiso4F·eIF4B·PABP is both enthalpy- and entropy-favorable. The ΔG values (Table 2) at 25 °C were calculated from eq 4. The ΔG values for the binding of eIFiso4F complexes with VPg were similar; however, the data suggest different forces driving the interaction. The eIFiso4F−VPg interaction is both enthalpically (77%) and entropically (24%) favorable, with a 53% greater enthalpic contribution to ΔG at 25 °C. This suggests hydrophobic interactions may play a role in binding either directly with the VPg or through conformational changes in the initiation factor complex. Addition of eIF4B has little effect on the enthalpic and entropic contribution of binding of eIFiso4F to VPg. PABP increases the enthalpic contribution ~92% and reduces the entropic contribution to ~8% for binding of eIFiso4F and eIFiso4F·4B to VPg. These data suggest that poly(A)-binding protein induces a conformational change in the protein complex, resulting in weakened hydrophobic interactions and strengthened hydrogen bonding, which could increase the specificity of the interactions.

PABP Increases the Kinetic Rate of eIFiso4F and eIFiso4F·4B with VPg. Stopped-flow kinetics for the binding of eIFiso4F with VPg has been previously determined.[14] To

dx.doi.org/10.1021/bi201929h | Biochemistry 2012, 51, 1388−1395

Table 1. Equilibrium Dissociation Constants (K_d) for the Interaction of eIFiso4F and eIFiso4F Complexes with VPg

complex	K_d (nM) at 5 °C	at 10 °C	at 15 °C	at 25 °C
eIFiso4F-VPg[a]	30.5 ± 0.4	39.2 ± 0.3	47.9 ± 0.4	81.3 ± 2.4
eIFiso4F·PABP-VPg	14.2 ± 0.3	18.1 ± 0.5	22.0 ± 2.0	29.4 ± 2.0
eIFiso4F·4B-VPg	28.2 ± 2.3	37.3 ± 3.4	46.1 ± 4.3	77.6 ± 5.5
eIFiso4F·4B·PABP-VPg	12.1 ± 0.6	15.5 ± 1.1	19.0 ± 0.9	24.3 ± 1.6
PABP-VPg				1789 ± 97

[a]Values from ref 13.

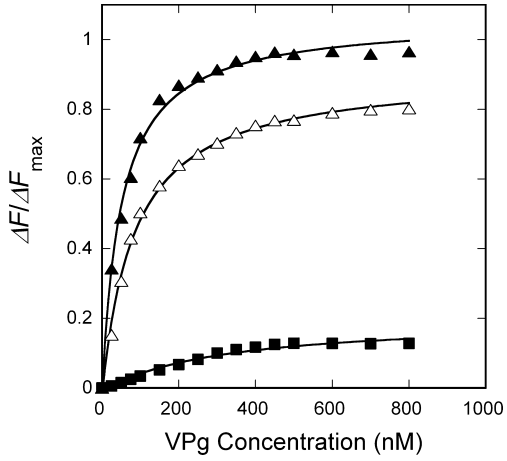

Figure 2. Poly(A)-binding protein affects the binding of eIFiso4F·4B to VPg. Fluorescence intensity measurements for the binding of eIFiso4F·4B (△), eIFiso4F·4B·PABP (▲), and eIF4B (■) with VPg. Experimental conditions were as described in the legend of Figure 1. The solid lines are the fitted curves. eIFiso4F·4B (1:10) and eIFiso4F·4B·PABP (1:10:30) complexes were prepared by incubation of 1 μM eIFiso4F, 10 μM eIF4B, and 30 μM PABP for 15 min at 4 °C, and 90% (eIFiso4F·4B) and 95% (eIFiso4F·4B·PABP) of the eIFiso4F were associated in the complex.

Table 2. Thermodynamic Parameters of Enthalpy, Entropy, and Free Energy Change for the Interactions of eIFiso4F and eIFiso4F Complexes with VPg

complex	ΔH (kJ/mol)	ΔS (J mol^{-1} K^{-1})	ΔG (kJ/mol)
eIFiso4F-VPg[a]	−31.0 ± 0.2	32.3 ± 0.4	−40.5 ± 0.5
eIFiso4F·4B-VPg	−32.1 ± 1.3	29.0 ± 3.0	−40.8 ± 0.8
eIFiso4F·PABP-VPg	−39.0 ± 2.4	11.5 ± 0.7	−42.5 ± 0.7
eIFiso4F·4B·PABP-VPg	−40.0 ± 2.0	11.2 ± 1.2	−42.6 ± 0.9

[a]Values from ref 13.

examine the role of VPg in cap-independent viral translation, we further investigated the kinetics of VPg with eIFiso4F in the presence of eIF4B and PABP. Time course data were fit by nonlinear regression analysis[35] as a single exponential as described in Experimental Procedures; a double exponential did not improve fits. Addition of PABP to eIFiso4F increased the rate constant (k_2) for VPg binding ~2.3-fold (eIFiso4F-VPg, k_2 = 69.0 ± 1.5 s^{-1}; eIFiso4F·PABP-VPg, k_2 = 159 ± 10 s^{-1}) at 22 °C (Figure 4 and Table 3). The addition of eIF4B did not affect the kinetic rate of binding of eIFiso4F to VPg (Figure 4 and Table 3) at the same temperature. However, at a lower temperature (5 °C), eIF4B enhanced binding rates by 2-fold and PABP enhanced the binding of eIFiso4F to VPg 4-fold, suggesting more stabilized complex formation at lower temperatures.

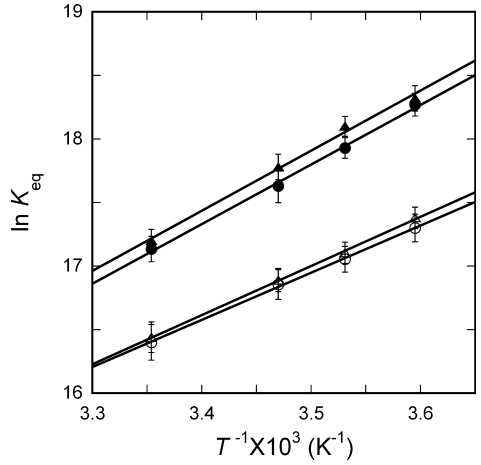

Figure 3. van't Hoff plots for the interaction of eIFiso4F with VPg in the presence of PABP and eIF4B. Data for eIFiso4F (○), eIFiso4F·PABP (●), eIFiso4F·4B (△), and eIFiso4F·4B·PABP (▲) with VPg. The enthalpy and entropy were determined from the slope and intercept, respectively, of the temperature-dependent equilibrium binding measurements.

Under pseudo-first-order conditions, where VPg was in excess, the observed rate constant was predicted to be a linear function of VPg concentration. However, as observed previously,[13,14] the binding rates show little dependence on VPg concentration over a concentration range of 2.5−10 μM, which constitutes a 10−40-fold excess (Figure 5). The observed rate varied from 151 to 167 s^{-1} for the eIFiso4F·PABP complex and from 172 to 184 s^{-1} for the eIFiso4F·4B·PABP complex with VPg. The mechanisms considered involved a one- and two-step binding process.[36,37]

$$\text{eIFiso4F} + \text{VPg} \underset{k_{-1}}{\overset{k_1}{\rightleftharpoons}} \text{eIFiso4F-VPg} \qquad \text{(mechanism 1)}$$

where k_1 and k_{-1} are the forward and reverse rate constants, respectively. Under the pseudo-first-order condition, the observed rate constant is predicted to be a linear function of substrate concentration; i.e., $k_{obs} = k_1[C] + k_{-1}$.

The two-step reaction is as follows:

$$\text{eIFiso4F} + \text{VPg} \underset{k_{-1}}{\overset{k_1}{\rightleftharpoons}} (\text{eIFiso4F-VPg})^* \underset{k_{-2}}{\overset{k_2}{\rightleftharpoons}} \text{eIFiso4F-VPg} \qquad \text{(mechanism 2)}$$

which involves a fast association of eIFiso4F and VPg followed by a slow change of conformation of the first association complex, (eIFiso4F-VPg)*, to the stable complex, eIFiso4F-VPg, giving rise to the fluorescence change.

The binding rates have the following relationship with respect to the concentration of substrate: $1/k_{obs} = 1/k_2 + k_1/k_2[C]$ as

dx.doi.org/10.1021/bi201929h | Biochemistry 2012, 51, 1388−1395

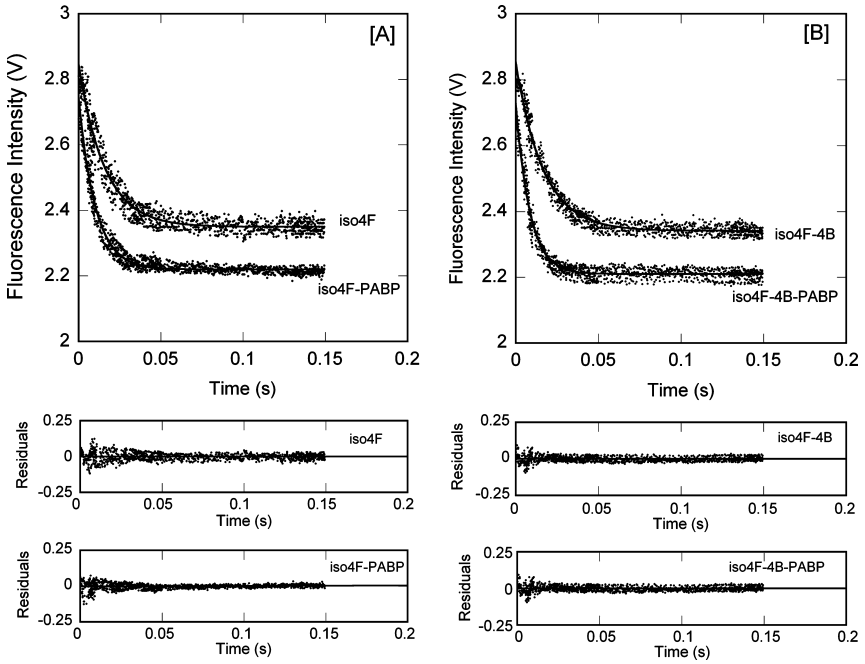

Figure 4. Poly(A)-binding protein increases the kinetic rates for the binding of eIFiso4F and eIFiso4F·4B with VPg. Typical time course of the intrinsic protein fluorescence intensity decrease caused by binding of VPg with (A) eIFiso4F and eIFiso4F·PABP or (B) eIFiso4F·4B and eIFiso4F·4B·PABP. A solution of 250 nM (final concentration) eIFiso4F, eIFiso4F·4B, or eIFiso4F·4B·PABP complex was rapidly mixed with 2.5 μM (final concentration) VPg at 22 °C. The solid line represents the fitted curve for a single-exponential function. Residuals for the fits are shown in the bottom panels. The excitation wavelength was 280 nm. The signal represents the total fluorescence emission above 320 nm. The experimental conditions are described in Experimental Procedures.

Table 3. Kinetic Rate Constants for the Interaction of eIFiso4F and eIFiso4F Complexes with VPg

	rate constant, k_2 (s^{-1})			
temp (°C)	eIFiso4F[a]	eIFiso4F	eIFiso4F·PABP	eIFiso4F·4B·PABP
5	7.03 ± 0.4	13.2 ± 0.7	28.1 ± 0.9	43.6 ± 2.7
10	13.0 ± 0.5	23.7 ± 1.1	56.9 ± 3.2	69.3 ± 3.3
15	25.0 ± 0.7	35.9 ± 2.3	95.6 ± 5.7	105 ± 5.6
22	69.0 ± 1.5	76.4 ± 3.3	159 ± 9.9	182 ± 9.0
E_a (kJ/mol)	81.0 ± 3.0	73.2 ± 3.3	61.0 ± 2.9	44.0 ± 2.4
dissociation rate k_{-2} ($\times 10^3$ s^{-1})	19.0 ± 0.9	13.2 ± 1.1	10.1 ± 0.7	6.5 ± 0.43

[a]Values from refs 13 and 14.

described previously,[35] where k_{obs} is the observed first-order rate constant, k_2 is the forward rate constant for the second step, and [C] is the concentration of VPg. Figure 5 shows $1/k_{obs}$ versus 1/[C] for eIFiso4F and the eIFiso4F complex, which shows a linear relationship. From the intercept of 1/[C] versus $1/k_{obs}$, k_2 was found to be 175 ± 4.0 and 188 ± 6.0 s^{-1} for eIFiso4F·PABP and eIFiso4F·4B·PABP, respectively.

Rate constants for binding of eIFiso4F and the eIFiso4F complex to VPg at different temperatures are listed in Table 3. The k_2 values for binding of VPg to the eIFiso4F complex at different temperatures were calculated from the data sets collected at each temperature. Addition of PABP to eIFiso4F or eIFiso4F·4B with VPg increased k_2 values. Similarly, the k_2 values for the eIFiso4F complexes increased with an increase in temperature (Table 3). The stopped-flow kinetic data showed that the binding of eIFiso4F·4B·PABP to VPg was approximately 2.5 times faster than the binding of eIFiso4F alone at 22 °C (Table 3 and Figure 4). The rate constant values as a function of temperature were used to construct an Arrehenius plot (Figure 6) according to eq 5. The activation energies were calculated from the slope of the fitted linear line of ln k versus $1/T$ (kelvin). Addition of PABP and eIF4B together lowers the activation energy ~2-fold for the binding of eIFiso4F with VPg as compared to eIFiso4F alone (Table 3) (eIFiso4F·4B·PABP-VPg, E_a = 44.0 ± 2.4 kJ/mol; eIFiso4F-VPg, E_a = 81.0 ± 3.0 kJ/mol).

Figure 7 shows the results of the dilution experiment described in Experimental Procedures. The dissociation rate constants were obtained from the fitted curves. Equilibrium calculations showed that less than 5% of the proteins remained as a complex after dilution, so that the reverse reaction could be neglected. Data fitting using a relaxation expression did not improve the quality of the fit. Addition of PABP to eIFiso4F decreased the dissociation rate ~2-fold for VPg (Table 3). However, PABP and eIF4B together decreased the dissociation rate ~3-fold as compared to eIFiso4F alone binding to VPg (Table 3).

DISCUSSION

Experiments were undertaken to investigate the extent to which poly(A)-binding protein and eIF4B affected binding of

dx.doi.org/10.1021/bi201929h | Biochemistry 2012, 51, 1388–1395

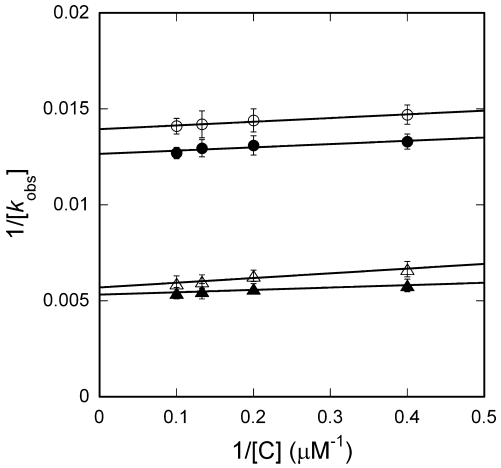

Figure 5. Kinetic plots of $1/k_{obs}$ vs $1/[C]$ for the interaction of eIFiso4F with VPg in the presence of eIF4B and PABP. Data for eIFiso4F (○), eIFiso4F·4B (●), eIFiso4F·PABP (△), and eIFiso4F·4B·PABP (▲) (250 nM each, final concentrations) with varying concentrations of VPg (2.5, 5, 7.5, and 10 μM, final concentrations). Rate constant k_2 was obtained as the reciprocal of the y intercept.

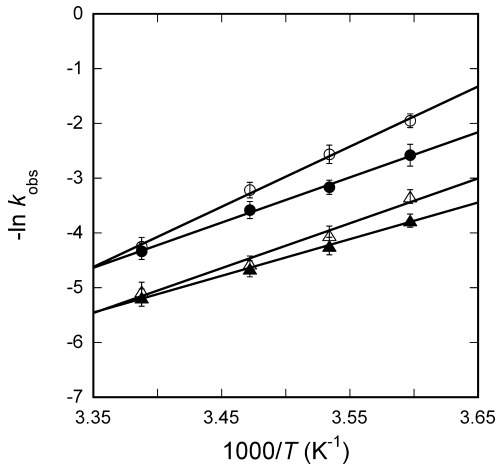

Figure 6. Determination of activation energies for the interaction of eIFiso4F with VPg in the presence of eIF4B and PABP using Arrhenius plots. The observed rate constant values for eIFiso4F (○), eIFiso4F·4B (●), eIFiso4F·PABP (△), and eIFiso4F·4B·PABP (▲) with VPg at different temperatures were used to construct an Arrhenius plot according to eq 5. The activation energy was calculated from the slope of the fitted linear plot of ln k vs $1/T$ (kelvin).

eIFiso4F to VPg of turnip mosaic virus. It has been demonstrated that VPg interacts with eIFiso4F,[13,14] and the interaction of the initiation factor with VPg is necessary for the infectivity of the virus.[16] In this study, we have shown that PABP increases the binding affinity of eIFiso4F and eIFiso4F·4B with VPg more than 2-fold, as compared to that of eIFiso4F alone. In contrast, PABP increased cap binding affinity by 40-fold for eIFiso4F.[38] However, the binding constant for VPg (0.081 μM), even in the absence of PABP, is significantly smaller than those for cap or capped oligonucleotide binding (8.9 and 3.7 μM, respectively).[39] This suggests that VPg can effectively compete with cap for eIFiso4F binding in the absence of PABP. In the presence of PABP, VPg binds to eIFiso4F ~7-fold more tightly than the cap in terms of equilibrium stability [K_d = 29.4 nM for eIFiso4F·PABP-VPg complex (Table 1), and K_d = 200 nM for eIFiso4F·PABP-Ant-m^{7}G cap[38]]. These results suggest that

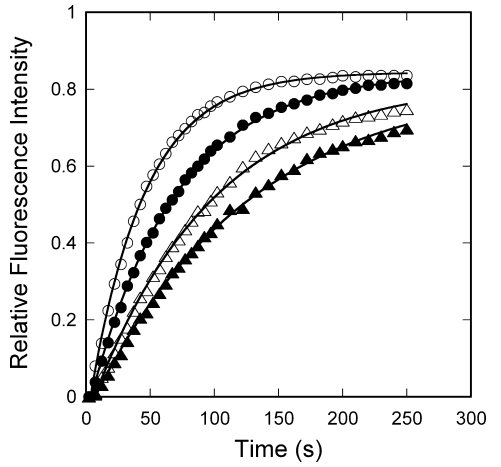

Figure 7. Kinetics of dissociation of VPg from eIFiso4F-VPg, eIFiso4F·4B-VPg, eIFiso4F·PABP-VPg, and eIFiso4F·4B·PABP-VPg complexes. Off rates for eIFiso4F-VPg (○), eIFiso4F·4B-VPg (●), eIFiso4F·PABP-VPg (△), and eIFiso4F·4B·PABP-VPg (▲) complexes were monitored by rapidly diluting 100 μL of the complex with 1500 μL of buffer at 25 °C. The concentrations of reactants before mixing were as follows: 2 μM VPg and 0.5 μM eIFiso4F, eIFiso4F·4B, eIFiso4F·PABP, or eIFiso4F·4B·PABP complex.

PABP stabilizes the formation of the initiation factor complex with VPg. PABP significantly changes the enthalpic and entropic contributions for the binding of eIFiso4F with VPg. The ΔH and ΔS values for the binding of the eIFiso4F·4B·PABP complex with VPg were −40.0 ± 2.0 kJ/mol and 11.2 ± 0.6 J mol^{-1} K^{-1}, respectively, whereas for binding of eIFiso4F to VPg, the values were reported to be −31.0 ± 0.2 kJ/mol and 32.3 ± 0.4 J mol^{-1} K^{-1}, respectively.[13] Binding of eIFiso4F·4B·PABP and eIFiso4F to VPg is 92 and 77% enthalpy-driven, respectively, with a large negative ΔH and a small positive ΔS. The thermodynamic data suggest a decrease in the level of hydrophobic interactions and an increase in the number of hydrogen bonds. The results suggest that binding of PABP to eIFiso4F and/or the eIFiso4F·4B complex induces a conformational change in eIFiso4F. Such a conformational change may result in increased specificity for VPg.

The mechanism of interaction of VPg with eIFiso4F·PABP and eIFiso4F·4B·PABP is consistent with our previous two-step binding mechanism[14] for the interaction of VPg with eIFiso4F. The kinetic data favor formation of a stable eIFiso4F·4B·PABP-VPg complex, and the rates indicate a mechanism by which VPg could kinetically compete with cap for eIFiso4F binding.[13] Our previous[13] study showed that binding of VPg with eIFiso4F was 2-fold faster than binding of eIFiso4F to Ant-m^{7}G cap.[36] Interestingly, PABP and eIF4B have a stronger effect on the binding of VPg to eIFiso4F than the binding of cap to eIFiso4F. VPg binding rates were enhanced 4-fold when both PABP and eIF4B were present, whereas cap binding rates were enhanced ~3-fold when both proteins were present[36] as compared to that of eIFiso4F alone at 22 °C. A significant difference in the association and dissociation rates is seen in the presence of PABP and eIF4B for the binding of eIFiso4F and VPg. Association rates for the binding of eIFiso4F with VPg in the presence and absence of eIF4B and PABP are faster than those for binding of initiation factors to cap.[36] However, dissociation rates are slower for the binding of initiation factors with VPg as compared to those with cap.[36] These data suggest that VPg more rapidly forms a stable complex with eIFiso4F in the presence of PABP and eIF4B than

dx.doi.org/10.1021/bi201929h | *Biochemistry* 2012, 51, 1388−1395

with the cap. A previous study using a GST pull-down assay, surface plasmon resonance, and isothermal calorimetric titration[40] has shown that binding of yeast eIF4E promotes a conformational change in eIF4G and leads to enhanced association with cap, which is necessary for the growth and maintenance of polysomes in vivo. PABP further stabilized the eIF4F complex via conformational changes. These studies suggest that PABP promotes conformational changes for the binding of eIFiso4F with VPg similar to those observed for cap binding.

Addition of PABP to eIFiso4F and eIFiso4F·4B reduced by almost half the activation energy as compared to our previous data[13] for binding of eIFiso4F alone to VPg, providing a path with a substantially lower energy barrier. However, the eIFiso4F·4B·PABP complex binds to VPg with an activation energy lower than that for binding of cap to the eIFiso4F·4B·PABP complex.[36] These data suggest that the combination of PABP and eIF4B produces a complex that not only has low activation energy but also maintains a rapid binding of VPg to the initiation complex as compared to cap binding. These studies suggest that VPg competes with cap for host cell initiation factors and VPg has a kinetic advantage over cap binding.

AUTHOR INFORMATION

Corresponding Author

*Department of Chemistry, Hunter College of the City University of New York, New York, NY 10065. Telephone: (212) 772-5383. Fax: (212) 772-5332. E-mail: dgoss@hunter.cuny.edu.

Funding

This work was supported in part by National Science Foundation Grants MCB 0814051 and MCB 1118320 (to D.J.G.).

Notes

The authors declare no competing financial interest.

ACKNOWLEDGMENTS

We thank Dr. Daniel R. Gallie (University of California, Riverside, CA) for the PABP clone, Dr. Karen Browning (University of Texas, Austin, TX) for the eIF4B clone, Dr. Hiroshi Miyoshi (St. Marianna University, Kawasaki, Japan) for the VPg clone, and Dr. John H. Trujillo for critical reading of the manuscript.

ABBREVIATIONS

VPg, viral protein linked to the genome; TuMV, turnip mosaic virus; UTR, untranslated region; eIF, eukaryotic initiation factor; PABP, poly(A)-binding protein; IRES, internal ribosomal entry sites; m^{7}GTP, 7-methylguanosine triphosphate.

REFERENCES

(1) Kahvejian, A., Svitkin, Y. V., Sukarieh, R., M'Boutchou, M. N., and Sonenberg, N. (2005) Mammalian poly(A)-binding protein is a eukaryotic translation initiation factor, which acts via multiple mechanisms. *Genes Dev. 19*, 104−113.

(2) Browning, K. S., Webster, C., Roberts, J. K., and Ravel, J. M. (1992) Identification of an isozyme form of protein synthesis initiation factor 4F in plants. *J. Biol. Chem. 267*, 10096−10100.

(3) Browning, K. S., Lax, S. R., and Ravel, J. M. (1987) Identification of two messenger RNA cap binding proteins in wheat germ. Evidence that the 28-kDa subunit of eIF-4B and the 26-kDa subunit of eIF-4F are antigenically distinct polypeptides. *J. Biol. Chem. 262*, 11228−11232.

(4) Gingras, A. C., Raught, B., and Sonenberg, N. (1999) eIF4 initiation factors: Effectors of mRNA recruitment to ribosomes and regulators of translation. *Annu. Rev. Biochem. 68*, 913−963.

(5) Abramson, R. D., Browning, K. S., Dever, T. E., Lawson, T. G., Thach, R. E., Ravel, J. M., and Merrick, W. C. (1988) Initiation factors that bind mRNA. A comparison of mammalian factors with wheat germ factors. *J. Biol. Chem. 263*, 5462−5467.

(6) Le, H., Tanguay, R. L., Balasta, M. L., Wei, C. C., Browning, K. S., Metz, A. M., Goss, D. J., and Gallie, D. R. (1997) Translation initiation factors eIF-iso4G and eIF-4B interact with the poly(A)-binding protein and increase its RNA binding activity. *J. Biol. Chem. 272*, 16247−16255.

(7) Tarun, S. Z. Jr., and Sachs, A. B. (1996) Association of the yeast poly(A) tail binding protein with translation initiation factor eIF-4G. *EMBO J. 15*, 7168−7177.

(8) Merrick, W. C. (1992) Mechanism and regulation of eukaryotic protein synthesis. *Microbiol. Rev. 56*, 291−315.

(9) Hershey, J. W. B., and Merrick, W. C. (2000) The pathway and mechanism of initiation of protein synthesis. In *Translational Control of Gene Expression*, Cold Spring Harbor Laboratory Press, Plainview, NY.

(10) Morley, S. J. (2001) The regulation of eIF4F during cell growth and cell death. In *Signaling pathway for translation*, Springer-Verlag, Berlin.

(11) Gallie, D. R. (1998) A tale of two termini: A functional interaction between the termini of an mRNA is a prerequisite for efficient translation initiation. *Gene 216*, 1−11.

(12) Wells, S. E., Hillner, P. E., Vale, R. D., and Sachs, A. B. (1998) Circularization of mRNA by eukaryotic translation initiation factors. *Mol. Cell 2*, 135−140.

(13) Khan, M. A., Miyoshi, H., Ray, S., Natsuaki, T., Suehiro, N., and Goss, D. J. (2006) Interaction of genome-linked protein (VPg) of turnip mosaic virus with wheat germ translation initiation factors eIFiso4E and eIFiso4F. *J. Biol. Chem. 281*, 28002−28010.

(14) Khan, M. A., Miyoshi, H., Gallie, D. R., and Goss, D. J. (2008) Potyvirus genome-linked protein, VPg, directly affects wheat germ in vitro translation: Interactions with translation initiation factors eIF4F and eIFiso4F. *J. Biol. Chem. 283*, 1340−1349.

(15) Grzela, R., Strokovska, L., Andrieu, J. P., Dublet, B., Zagorski, W., and Chroboczek, J. (2006) Potyvirus terminal protein VPg, effector of host eukaryotic initiation factor eIF4E. *Biochimie 88*, 887−896.

(16) Leonard, S., Plante, D., Wittmann, S., Daigneault, N., Fortin, M. G., and Laliberte, J. F. (2000) Complex formation between potyvirus VPg and translation eukaryotic initiation factor 4E correlates with virus infectivity. *J. Virol. 74*, 7730−7737.

(17) Robaglia, C., and Caranta, C. (2006) Translation initiation factors: A weak link in plant RNA virus infection. *Trends Plant Sci. 11*, 40−45.

(18) Miyoshi, H., Suehiro, N., Tomoo, K., Muto, S., Takahashi, T., Tsukamoto, T., Ohmori, T., and Natsuaki, T. (2006) Binding analyses for the interaction between plant virus genome-linked protein (VPg) and plant translational initiation factors. *Biochimie 88*, 329−340.

(19) Dunoyer, P., Thomas, C., Harrison, S., Revers, F., and Maule, A. (2004) A cysteine-rich plant protein potentiates Potyvirus movement through an interaction with the virus genome-linked protein VPg. *J. Virol. 78*, 2301−2309.

(20) Schaad, M. C., Lellis, A. D., and Carrington, J. C. (1997) VPg of tobacco etch potyvirus is a host genotype-specific determinant for long-distance movement. *J. Virol. 71*, 8624−8631.

(21) Rajamaki, M. L., and Valkonen, J. P. (2002) Viral genome-linked protein (VPg) controls accumulation and phloem-loading of a potyvirus in inoculated potato leaves. *Mol. Plant-Microbe Interact. 15*, 138−149.

(22) Keller, K. E., Johansen, I. E., Martin, R. R., and Hampton, R. O. (1998) Potyvirus genome-linked protein (VPg) determines pea seed-borne mosaic virus pathotype-specific virulence in *Pisum sativum*. *Mol. Plant-Microbe Interact. 11*, 124−130.

(23) Nicolas, O., Dunnington, S. W., Gotow, L. F., Pirone, T. P., and Hellmann, G. M. (1997) Variations in the VPg protein allow a

potyvirus to overcome va gene resistance in tobacco. *Virology 237*, 452−459.
(24) Hong, Y., Levay, K., Murphy, J. F., Klein, P. G., Shaw, J. G., and Hunt, A. G. (1995) A potyvirus polymerase interacts with the viral coat protein and VPg in yeast cells. *Virology 214*, 159−166.
(25) Li, X. H., Valdez, P., Olvera, R. E., and Carrington, J. C. (1997) Functions of the tobacco etch virus RNA polymerase (NIb): Subcellular transport and protein-protein interaction with VPg/proteinase (NIa). *J. Virol. 71*, 1598−1607.
(26) Fellers, J., Wan, J., Hong, Y., Collins, G. B., and Hunt, A. G. (1998) In vitro interactions between a potyvirus-encoded, genome-linked protein and RNA-dependent RNA polymerase. *J. Gen. Virol. 79* (Part 8), 2043−2049.
(27) Suehiro, N., Natsuaki, T., Watanabe, T., and Okuda, S. (2004) An important determinant of the ability of turnip mosaic virus to infect *Brassica* spp. and/or *Raphanus sativus* is in its P3 protein. *J. Gen. Virol. 85*, 2087−2098.
(28) van Heerden, A., and Browning, K. S. (1994) Expression in *Escherichia coli* of the two subunits of the isozyme form of wheat germ protein synthesis initiation factor 4F. Purification of the subunits and formation of an enzymatically active complex. *J. Biol. Chem. 269*, 17454−17457.
(29) Khan, M. A., Yumak, H., Gallie, D. R., and Goss, D. J. (2008) Effects of poly(A)-binding protein on the interactions of translation initiation factor eIF4F and eIF4F·4B with internal ribosome entry site (IRES) of tobacco etch virus RNA. *Biochim. Biophys. Acta 1779*, 622−627.
(30) Cheng, S., and Gallie, D. R. (2007) eIF4G, eIFiso4G, and eIF4B bind the poly(A)-binding protein through overlapping sites within the RNA recognition motif domains. *J. Biol. Chem. 282*, 25247−25258.
(31) Bradford, M. M. (1976) A rapid and sensitive method for the quantitation of microgram quantities of protein utilizing the principle of protein-dye binding. *Anal. Biochem. 72*, 248−254.
(32) Firpo, M. A., Connelly, M. B., Goss, D. J., and Dahlberg, A. E. (1996) Mutations at two invariant nucleotides in the 3′-minor domain of *Escherichia coli* 16 S rRNA affecting translational initiation and initiation factor 3 function. *J. Biol. Chem. 271*, 4693−4698.
(33) Khan, M. A., and Goss, D. J. (2004) Phosphorylation states of translational initiation factors affect mRNA cap binding in wheat. *Biochemistry 43*, 9092−9097.
(34) Khan, M. A., Yumak, H., and Goss, D. J. (2009) Kinetic mechanism for the binding of eIF4F and tobacco etch virus internal ribosome entry site RNA: Effects of eIF4B and poly(A)-binding protein. *J. Biol. Chem. 284*, 35461−35470.
(35) Olsen, K., Christensen, U., Sierks, M. R., and Svensson, B. (1993) Reaction mechanisms of Trp120 → Phe and wild-type glucoamylases from *Aspergillus niger*. Interactions with maltooligodextrins and acarbose. *Biochemistry 32*, 9686−9693.
(36) Khan, M. A., and Goss, D. J. (2005) Translation initiation factor (eIF) 4B affects the rates of binding of the mRNA m7G cap analogue to wheat germ eIFiso4F and eIFiso4F·PABP. *Biochemistry 44*, 4510−4516.
(37) Garland, D. L. (1978) Kinetics and mechanism of colchicine binding to tubulin: Evidence for ligand-induced conformational change. *Biochemistry 17*, 4266−4272.
(38) Wei, C.-C., Balasta, M. L., Ren, J., and Goss, D. J. (1998) Wheat germ poly(A) binding protein enhances the binding affinity of eukaryotic initiation factor 4F and (iso)4F for cap analogs. *Biochemistry 37*, 1910−1916.
(39) Carberry, S. E., and Goss, D. J. (1991) Wheat germ initiation factors 4F and (iso)4F interact differently with oligoribonucleotide analogues of rabbit α-globin mRNA. *Biochemistry 30*, 4542−4545.
(40) Gross, J. D., Moerke, N. J., von der Haar, T., Lugovskoy, A. A., Sachs, A. B., McCarthy, J. E., and Wagner, G. (2003) Ribosome loading onto the mRNA cap is driven by conformational coupling between eIF4G and eIF4E. *Cell 115*, 739−750.